Assessment of adsorption properties of inorganic–organic hybrid cyclomatrix type polyphosphazene microspheres for the removal of Pb(II) ions from aqueous solutions

Tuğba Alp Arıcı, Simge Metinoğlu Örüm, Yasemin Süzen Demircioğlu, Adnan Özcan & A. Safa Özcan

Published online: 08 Nov 2018.

Submit your article to this journal

Article views: 52

View Crossmark data

Taylor & Francis
Taylor & Francis Group

Check for updates

Assessment of adsorption properties of inorganic–organic hybrid cyclomatrix type polyphosphazene microspheres for the removal of Pb(II) ions from aqueous solutions

Tuğba Alp Arıcı[a], Simge Metinoğlu Örüm[b], Yasemin Süzen Demircioğlu[c], Adnan Özcan[c], and A. Safa Özcan[c]

[a]Department of Chemical Technology, Emet Vocational School, Dumlupınar University, Kütahya, Turkey; [b]Department of Chemistry, Faculty of Arts and Science, Mehmet Akif Ersoy University, Burdur, Turkey; [c]Department of Chemistry, Faculty of Science, Eskişehir Technical University, Eskişehir, Turkey

ABSTRACT

Inorganic–organic hybrid cyclomatrix type polyphosphazene microspheres (poly[cyclotriphosphazene-co-(4,4′-diaminodiphenylmethane)]) (HDMS) and poly[cyclotetraphosphazene-co-4,4′-diaminodiphenylmethane)] (ODMS) were prepared to investigate their possible use as alternative adsorbents for the comparative study on Pb(II) ions removal from aqueous solutions. The structures of the microspheres were elucidated by Fourier Transform Infrared (FTIR) spectroscopy and Dynamic Light Scattering (DLS) measurements, and the surface morphologies were also observed by Scanning Electron Microscopy (SEM). The adsorption of Pb(II) ions onto HDMS and ODMS from aqueous solutions was examined by means of pH, temperature, contact time and concentration. Furthermore, adsorption kinetics and isotherm models were applied and the experimental data fitted well with Langmuir isotherm and pseudo-second-order kinetic models. The maximum adsorption capacities of HDMS and ODMS for Pb(II) ions were obtained as 157.8 and 308.0 mg g^{-1} at 20 °C and pH 5.5, respectively.

GRAPHICAL ABSTRACT
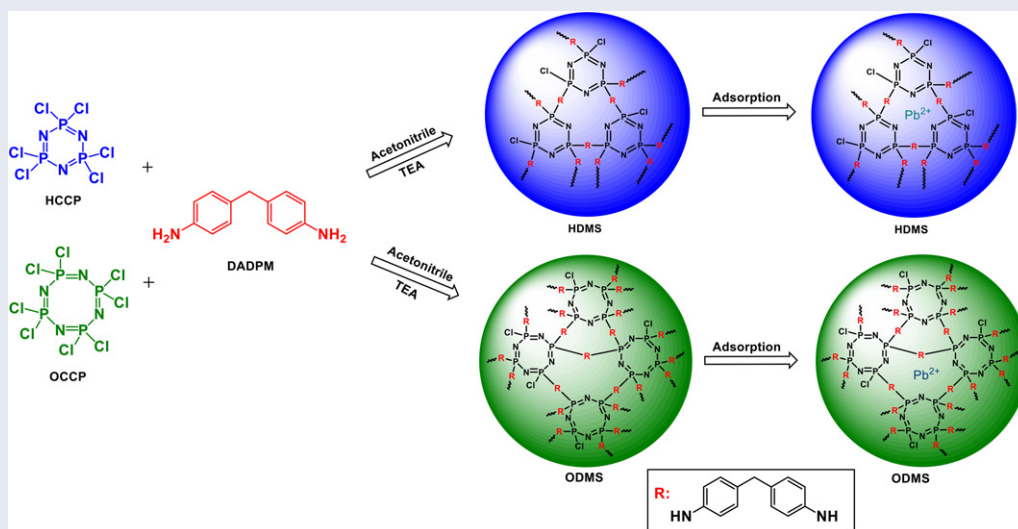
Introduction

With the development of industry, heavy metal pollutants have become one of the serious main problems for the environment. Toxic metal compounds not only contaminate surface waters but also pollute underground waters. The removal of heavy metal ions from wastewater is essential to protect public health due to fact that these metal ions are persistent and nondegradable in the environment.[1] Various methods such as adsorption, chemical coagulation, ion exchange and membrane separation process to eliminate toxic heavy metals from wastewater have been used for this aim. The adsorption process is an effective technique and

has been widely employed for the removal of heavy metals from wastewater.[2] To improve the efficiency of the adsorption process, developing effective adsorbents with higher adsorption capacities is essential.

The science of polyphosphazenes has arisen as a pivotal point of much research owing to their inherent backbone stability, interesting mechanical properties, specific chemical reactivity, structural diversity and ability to form inorganic–organic hybrid materials exhibiting desired properties because of flexible organic functional groups.[3,4] The nano- and micro-sized cross-linked polyphosphazene materials in the form of spheres, rods and fibers have been extensively explored due to their specific morphologies, impressive features and potential applications[3] and have been widely used as flame retardant materials,[5] membranes,[6] biomaterials,[7] drug delivery and controlled release systems,[8,9] adsorbents,[10,11] and optoelectrical materials.[12] Increasing efforts have been targeted to use inorganic–organic hybrid polyphosphazenes as adsorbents for the removal of harmful waste from aqueous solutions due to their controllable surface morphology, internal structures and modifiable functional groups.[13–16] Polyphosphazenes consist of an inorganic backbone (–P=N–) and organic side groups, attached to phosphorus atoms.[17] Cyclomatrix type polyphosphazenes are highly cross-linked polymers that are generally formed by the reaction of hexachlorocyclotriphosphazene (HCCP) and multifunctional phenol or amines via a one pot precipitation polymerization technique.[18,19]

Lead is one of the toxic heavy metals and discharges into the environment from dust storms, lead-acid battery industry, mining and smelting operations, battery recycling and industrial wastes.[20] The concentrations of Pb(II) ions in solutions should be restricted in the range of 0.1–0.05 mg dm^{-3}.[21] The large dosages of Pb(II) ions in the human body can cause hypertension, brain damage, abdominal pain, anemia, cramps, vomiting, nausea and learning disabilities.[22]

Different types of inorganic–organic hybrid cyclomatrix polyphosphazene microspheres, were chosen to investigate the possible use of polyphosphazene microspheres as alternative adsorbents for the removal of Pb(II) ions from aqueous solutions. Studied polyphosphazene microspheres, which are namely HDMS (poly(cyclotriphosphazene-co-4,4′-diaminodiphenylmethane) and ODMS (poly(cyclotetraphosphazene-co-4,4′-diaminodiphenylmethane), possess N-donor atoms in different numbers due to skeletal rings and functional groups. They were synthesized by using hexachlorocyclotriphosphazene

(HCCP) and octachlorocyclotetraphosphazene (OCCP) as crosslinkers and 4,4′-diaminodiphenylmethane (DADPM) as monomer via precipitation polymerization technique. Polyphosphazene based adsorbents were also preferred owing to a lack of information on their metal adsorption abilities. The effects of pH, temperature, contact time and concentration were examined for the adsorption of Pb(II) ions onto HDMS and ODMS. The adsorption kinetics and isotherm parameters were also evaluated from the experimental data.

Results and discussion

Preparation and characterization of HDMS and ODMS

Polyphosphazene microspheres (HDMS, poly(cyclotriphosphazene-co-4,4′-diaminodiphenylmethane and ODMS poly-(cyclotetraphosphazene-co-4,4′-diaminodiphenylmethane) were prepared by precipitation polymerization reaction of crosslinkers (HCCP, $N_3P_3Cl_6$; OCCP, $N_4P_4Cl_8$) and monomer (DADPM, 4,4′-diaminodiphenylmethane) in acetonitrile using excess amount of TEA, as an acid acceptor, by using ultrasonic power. The method were previously reported in the literature and also published by our group.[23–26] This synthesis route is simple and a one pot polycondensation technique without using any stabilizer and surfactant. Besides, hexachlorocyclotriphosphazene (HCCP, $N_3P_3Cl_6$) has been used as a crosslinker, widely studied molecule in polyphosphazene chemistry, to obtain cyclomatrix type polyphosphazene spheres.[27,28] On the contrary, there are few studies about skeletal flexible eight-membered ring octachlorocyclotetraphosphazene (OCCP, $N_4P_4Cl_8$).[29,30]

The surface morphologies of HDMS and ODMS are illustrated in Figure 1. It can be seen from the figure that the synthesized particles have spherical shape and smooth surface. The surface areas of HDMS and ODMS were found to be as 94.35 and 54.78 m^2 g^{-1}, respectively, by using the Methylene Blue method.

FTIR spectra were employed to verify the functional groups of the polyphosphazene microspheres and metal adsorbed polyphosphazene microspheres (Figures 2, 3). The absorption bands observed at 3371, 3152 and 1613 cm^{-1} for HDMS (Figure 2a), 3370, 3202 and 1612 cm^{-1} for Pb-loaded HDMS (Figure 2b) and 3425, 3041 and 1615 cm^{-1} for ODMS (Figure 3a), at 3364, 3188 and 1615 cm^{-1} for Pb-loaded ODMS (Figure 3b) represent to the N–H stretching and bending bands, indicating the presence of primary or
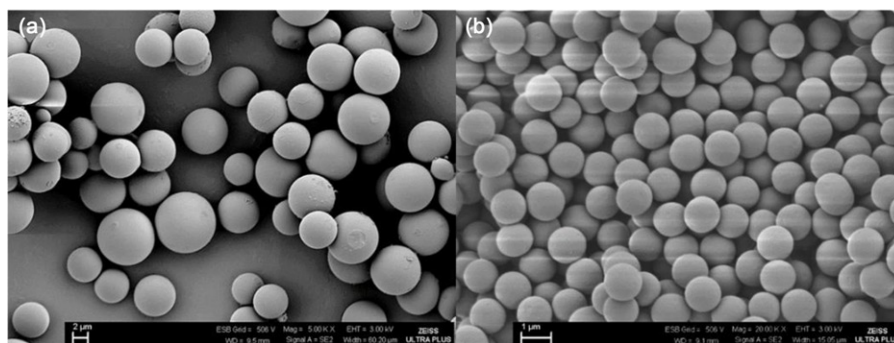

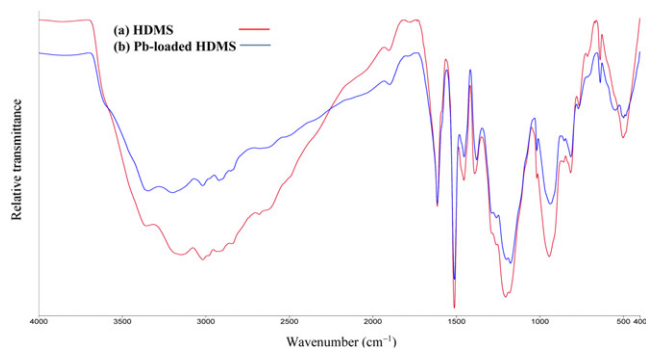**Figure 1.** SEM images of (a) HDMS and (b) ODMS.[25, 26]

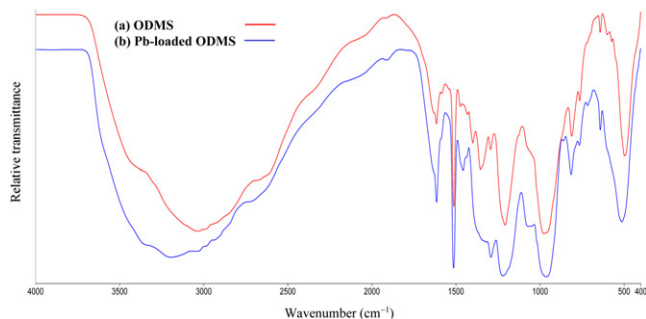**Figure 2.** FTIR spectra of HDMS before (a) and after (b) adsorption.

Figure 3. FTIR spectra of ODMS before (a) and after (b) adsorption.

Figure 4. The particle size distributions of HDMS and ODMS before and after adsorption.

secondary amine groups on the microspheres/loaded microspheres.[31] The aromatic C–H stretching vibrations bands of HDMS were observed at 3019 and 2973 cm^{-1}, 3019 and 2913 cm^{-1} for Pb-loaded HDMS (Figure 2a, b). The implied bands for ODMS were observed at 3042 and 2977 cm^{-1} and they were shifted to 3040 and 2986 cm^{-1} for Pb-loaded ODMS (Figure 3a, b) due to the adsorption of Pb(II) ions onto microspheres.[16] For HDMS and Pb-loaded HDMS, the C=C aromatic ring stretching and bending vibrations were observed at 1512, 760 and 1512, 774 cm^{-1}; and for ODMS and Pb-loaded ODMS they were obtained at 1512, 763 and 1513, 761 cm^{-1}, respectively.[11,14] The characteristic P=N and P–N absorption bands for HDMS and Pb-loaded HDMS were observed between 1295–1174 and 1286–1175 cm^{-1} and for ODMS and Pb-loaded ODMS they were around at 1207 and 1217 cm^{-1}.[14] The changes in absorption bands can be considered as an evidence for the adsorption of Pb(II) ions onto HDMS and ODMS.[25,26]

DLS measurements were performed to determine the particle sizes of the studied samples in water. The particle size distributions of the samples are depicted in Figure 4. The results indicated that particle size values for HDMS, Pb-loaded HDMS, ODMS and Pb-loaded ODMS were found to be as 3.85, 3.82, 1.08 and 1.04 μm, respectively. The reason for the similar particle size values obtained for both microspheres and Pb-loaded microspheres may be explained by interacting Pb(II) ions with interior N-donor atoms of the polyphosphazene microspheres.

Effect of pH on Pb(II) ions adsorption

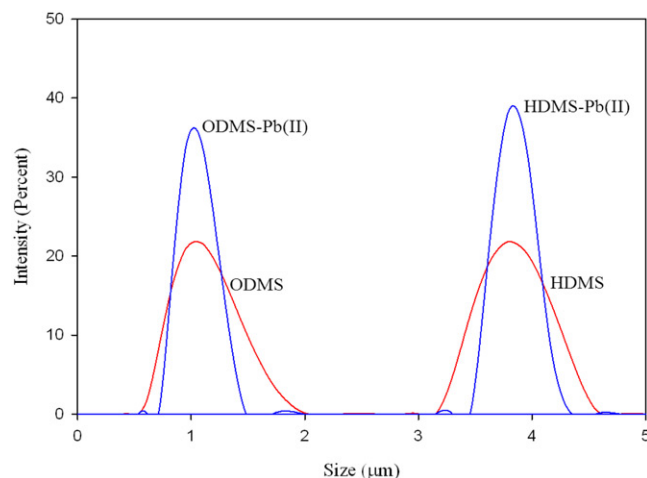pH is the most important parameter affecting the properties of adsorbents on the removal of heavy metal ions. The

influence of pH on the amount of adsorbed Pb(II) ions onto the adsorbents (HDMS and ODMS) was performed in the range of 1.0–6.0 (Figure 5). The adsorption capacity of Pb(II) ions from solution can be increased with an increase in pH values and reached the maximum amount at pH 5.5. It was observed that the adsorbed amounts changed from 19.4 to 109.7 mg g^{-1} for HDMS and from 40.6 to 169.8 mg g^{-1} for ODMS. Ineffective adsorption at acidic pH values may be attributed to the abundance of hydronium ions and ionic repulsion between the positively charged surface and the positive metal ions. The effective adsorption of Pb(II) ions onto HDMS and ODMS at pH 5.5 may be due to neutralization of the positively charged at the surfaces. Under this condition, ODMS displayed high adsorption performance that may be due to having more donor atoms to interact with Pb(II) ions and generate coordination complexes/chelates easily.[32]

Effect of temperature

To examine the effect of temperature, the experiments were conducted from 10 to 45 °C (Figure 6). The adsorption of Pb(II) ions onto the adsorbents was not remarkably effected by the temperature. The amounts of adsorbed Pb(II) ions were determined changing from 118.3 to 117.8 mg g^{-1} for HDMS and 184.5 to 180.2 mg g^{-1} for ODMS at the temperature range. The optimum temperature was preferred as 20 °C for further experiments.

Adsorption kinetics

The contact time on the adsorption process is an essential effect in order to obtain the information about adsorption mechanism. Active sites in adsorption were occupied and reached saturation with rising in time. Figure 7 displays the influence of contact time for Pb(II) ions removal by HDMS and ODMS. Since ODMS has a highly cross-linked polymeric structure and possesses a density of electron-rich groups, the adsorption of Pb(II) ions onto ODMS is higher than HDMS. The adsorption rate of Pb(II) ions was initially
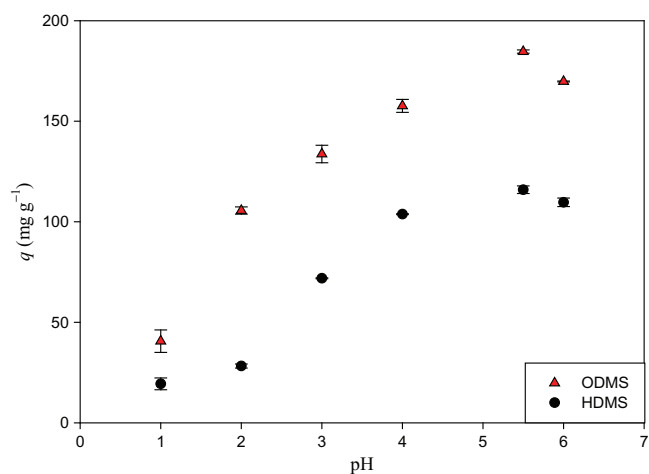
Figure 5. Effect of pH on the adsorption of Pb(II) ions onto HDMS and ODMS at 20 °C.
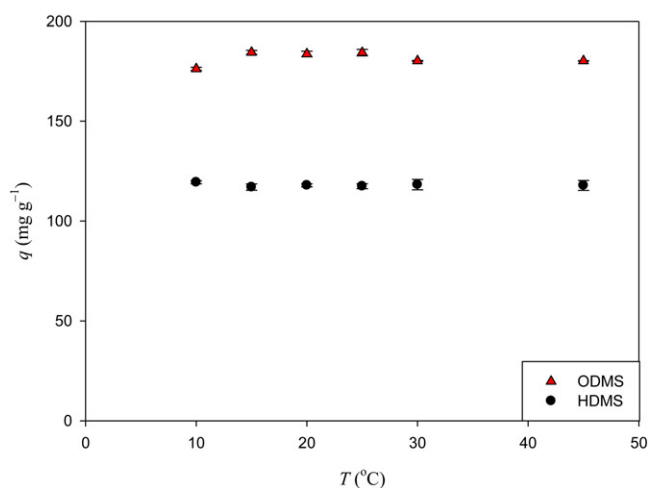

Figure 6. Effect of temperature on the adsorption of Pb(II) ions onto HDMS and ODMS.
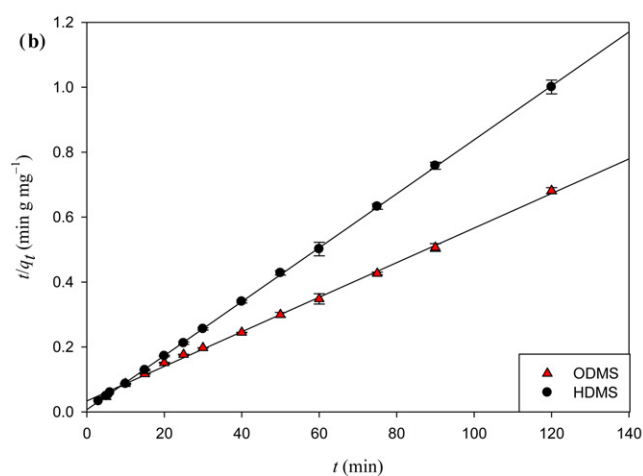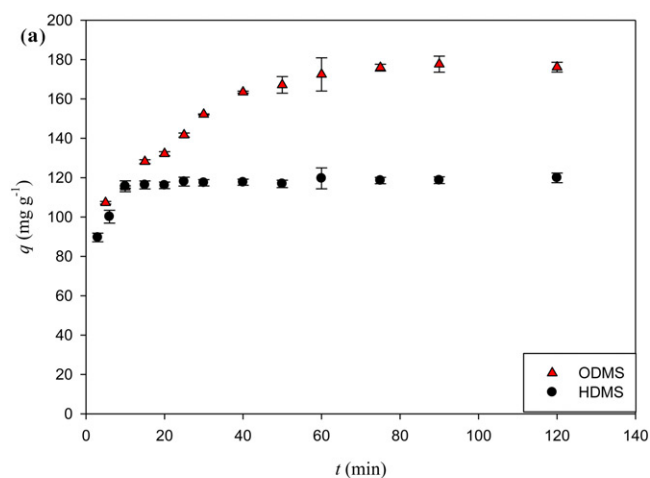

Figure 7. (a) The adsorption kinetics of Pb(II) ions onto HDMS and ODMS and (b) pseudo-second order kinetic plots for the adsorption of Pb(II) ions onto HDMS and ODMS (pH = 5.5; $t = 20$ °C; $C_o = 100$ mg dm^{-3}).

rapid and then slow down gradually and reached the equilibrium. It can be seen from the figure that the removal efficiency for HDMS increased sharply and reached equilibrium at 15 min, while ODMS required 50 min. After designated times, there was no considerable increase in the removal capacity of Pb(II) ions.

Four kinetic models including Lagergren first-order (Eq. 1),[33] pseudo-second-order (Eq. 2),[34,35] Elovich kinetic models (Eq. 3),[36] and intraparticle diffusion (Eq. 4)[37] equations have been employed to assist the experimental data to obtain information about adsorption mechanism. The equations for the models are expressed as following:

$$\ln(q_1 - q_t) = \ln q_1 - k_1 t \quad (1)$$

$$\frac{t}{q_t} = \frac{1}{k_2 q_2^2} + \frac{1}{q_2} t \quad (2)$$

$$q_t = \frac{1}{\beta} \ln(\alpha\beta) + \frac{1}{\beta} \ln t \quad (3)$$

$$q_t = k_p\, t^{1/2} + C \quad (4)$$

where q_1 and q_t are the amounts of adsorbed Pb(II) ions onto the adsorbent at the equilibrium and various times t (mg g^{-1}), k_1 is the rate constant of the Lagergren first-order model (min^{-1}), q_2 is the amount of Pb(II) ions at the equilibrium for the pseudo-second-order adsorption (mg g^{-1}), k_2 is the rate constant of the pseudo-second-order model (g mg^{-1} min^{-1}), α and β are initial adsorption rate (mg g^{-1} min^{-1}) and desorption constant (g mg^{-1}) for Elovich equation and C and k_p are intercept and intraparticle diffusion rate constant (mg g^{-1} min$^{-1/2}$) for the intraparticle diffusion model.

The linear plots of $\ln(q_1 - q_t)$ versus t for the Lagergren first-order kinetic model, t/q_t against t for the pseudo-second-order kinetic (Figure 7), the plots of q_t versus $\ln t$ for the Elovich kinetic and q_t against $t^{1/2}$ for the intraparticle diffusion models have been generated to the rate parameters. The kinetic parameters for the adsorption of Pb(II) ions onto HDMS and ODMS at 20 °C were determined from the related plots and are depicted in Table 1. The experimental data fitted well to the pseudo-second-order model with the highest correlation coefficient. The amounts of adsorbed Pb(II) ions at equilibrium were found to be 120.3 mg g^{-1} for HDMS and 187.8 mg g^{-1} for ODMS. These values were also compatible with obtained experimental values. Although

Table 1. The calculated kinetic parameters for the adsorption of Pb(II) ions onto HDMS and ODMS at 20 °C.

Adsorbent	Lagergren-first-order			Pseudo-second-order			Elovich			Intraparticle diffusion		
	q_1 (mg g^{-1})	k_1 (min^{-1})	r_1^2	q_2 (mg g^{-1})	k_2 (g mg^{-1} min^{-1})	r_2^2	α (mg g^{-1} min^{-1})	β (g mg^{-1})	r_E^2	C (mg g^{-1})	k_p (mg g^{-1} min$^{-1/2}$)	r_p^2
HDMS	10.3	3.00×10^{-2}	0.602	120.3 ± 0.732	1.02×10^{-2}	0.999	7.18×10^5	0.147	0.728	57.3	18.2	0.988
ODMS	79.1	3.89×10^{-2}	0.917	187.8 ± 7.156	8.38×10^{-4}	0.998	10.2	3.84×10^{-2}	0.956	74.6	13.6	0.977

poor fittings were exhibited for the Lagergren first-order, Elovich kinetic and the intraparticle diffusion models, the intraparticle diffusion model was evaluated more precisely for the adsorption of Pb(II) ions onto HDMS and ODMS. This model involves several steps: (1) bulk diffusion, (2) film diffusion, (3) intraparticle diffusion and (4) adsorption on an active site.[37] Multilinear plots for the experimental data of HDMS and ODMS were drawn. In the first step, a rapid adsorption (bulk diffusion; $C = 57.3$ for HDMS and $C = 74.6$ for ODMS) obtains and the intraparticle diffusion is not the only rate-controlling step, but also other processes may control the rate of adsorption, all of which may be operating simultaneously.[38] Further, the adsorption gradually decreases by second (film diffusion; $C = 112.4$ for HDMS and $C = 106.4$ for ODMS) and third (intraparticle diffusion; $C = 108.8$ for HDMS and $C = 149.4$ for ODMS) linear portions of the curve. Consequently, intraparticle diffusion has a part in the adsorption process. In the final step (adsorption step; $C = 113.1$ for HDMS and $C = 187.5$ for ODMS), the intraparticle diffusion decelerates because of low Pb(II) ions concentration in the solution.
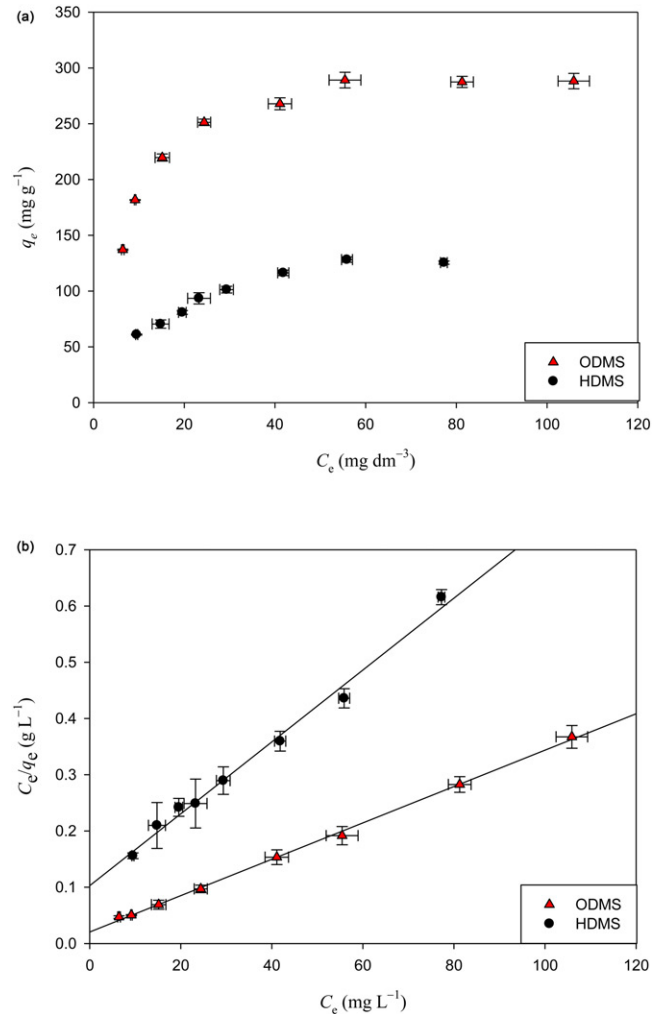
Adsorption isotherms

It is generally known that adsorption isotherms represent significant knowledge about adsorption characteristics and equilibrium data to describe adsorbate molecules how to interact with adsorbents. The adsorption capacity of the adsorbent, which is very substantial to draft adsorption systems, can be designated by the analysis of the isotherm data. The data obtained from the performed studies were interpreted by classical adsorption isotherm models (Figure 8). Langmuir, Freundlich and Dubinin–Radushkevich (D–R) isotherm models are utilized to determine the equilibrium between adsorbed Pb(II) ions on the adsorbents (HDMS or ODMS) and Pb(II) ions in solution at a constant temperature.

The Langmuir adsorption model supposes a monolayer adsorption onto a homogeneous adsorbent surface where all adsorption sites are identical and energetically equivalent. Langmuir adsorption isotherm applied to equilibrium adsorption and it comprises a limited number of active sites with homogeneous adsorption energy. The analysis of equilibrium data for the adsorption of Pb(II) ions onto the adsorbents (HDMS and ODMS) has been tested by the linear form (Eq. 5) of the Langmuir (1918)[39] isotherm equation.

$$\frac{C_e}{q_e} = \frac{1}{q_{max} K_L} + \frac{C_e}{q_{max}} \tag{5}$$

where q_e is the equilibrium metal ions concentration on the adsorbent (mg g^{-1}), C_e is the equilibrium metal ions concentration in the solution (mg dm^{-3}), q_{max} is the monolayer

Figure 8. (a) The adsorption isotherms of Pb(II) ions onto HDMS and ODMS and (b) Langmuir plots for the adsorption of Pb(II) ions onto HDMS and ODMS.

capacity of the adsorbent (mg g^{-1}) and K_L is the Langmuir adsorption constant (dm^3 mg^{-1}). A plot of C_e/q_e vs. C_e presents a linear graph (Figure 8) and, q_{max} and K_L were figured out from the slope and the intercept of the graph.

The convenience of the adsorption process was checked by applying a simple method. The nature of isotherm can be defined as linear, favorable or unfavorable by the attained value of separation factor (R_L, Eq. 6) as unity, between 0–1 and zero, respectively. In this manner, the Langmuir constant, K_L, can be employed to designate the practicability of the adsorbent for the removal of Pb(II) ions.[40,41]

$$R_L = \frac{1}{1 + K_L C_0} \tag{6}$$

Where C_o is the highest initial metal ions concentration (mg dm^{-3}).

The Freundlich isotherm is an empirical equation to explain heterogeneous systems. A linear form of the Freundlich equation (Eq. 7)[42] is

$$\ln q_e = \ln K_F + \frac{1}{n}\ln C_e \qquad (7)$$

where K_F (dm^3 g^{-1}) and n (dimensionless) are Freundlich adsorption isotherm constants. The plot of $\ln q_e$ vs. $\ln C_e$ for the adsorption of Pb(II) ions was used to calculate isotherm constants from the intercept and the slope values.

The Dubinin–Radushkevich (D–R) isotherm, which is a general isotherm, does not suppose a homogeneous surface or constant adsorption potentials. To reveal the discrimination between the physical and chemical adsorption, this isotherm model may be employed. The linear form of D–R isotherm equation (Eq. 8)[43] is

$$\ln q_e = \ln q_m - \beta\varepsilon^2 \qquad (8)$$

where β (mol^2 kJ^{-2}) is an isotherm constant, q_m is the maximum adsorption capacity, and ε is the Polanyi potential, which can be calculated by $RT\ln(1+\frac{1}{C_e})$. To attain the values of q_m and β, the plot of $\ln q_e$ against ε^2 is drawn.

The constant β employs to calculate the mean free energy E (kJ mol^{-1}) of adsorption per molecule of the adsorbate and it can be expressed as following (Eq. 9):[44,45]

$$E = \frac{1}{(2\beta)^{1/2}} \qquad (9)$$

When the amount of E is between 8 and 16 kJ mol^{-1}, it can be designated that the process obeys by a chemical adsorption.[46] The value of E should be smaller than 8 kJ mol^{-1}, for a physical adsorption.[47]

The calculated isotherm parameters are recorded in Table 2. According to the results, the correlation coefficient (r_L^2) for the Langmuir model appears to be the highest in comparison with the other isotherm models. The calculated values of R_L for HDMS and ODMS were also found to be 0.105 and 2.15×10^{-2}, respectively. These results indicate

that the adsorption of Pb(II) ions onto HDMS and ODMS are favorable. The maximum adsorption capacities of HDMS and ODMS obtained for Pb(II) ions were 157.4 and 308.0 mg g^{-1} from the Langmuir adsorption isotherm model, respectively.

The Freundlich constant value of K_F at equilibrium were found to be 25.5 and 107.3 dm^3 g^{-1} for the adsorbents. The numerical values of n are 2.536 and 4.252 and they are greater than unity, indicating that Pb(II) ions are favorably adsorbed by HDMS and ODMS.

The mean free energy, E, (kJ mol^{-1}) of the adsorption was associated with D–R isotherm model and evaluated from Eq. (9). Based on the obtained E value, it is decided that the adsorption system is a physical or chemical process. Although the values of E for the adsorption of Pb(II) ions onto HDMS and ODMS were obtained as 11.62 and 14.86 kJ mol^{-1} which seem to fit in with a chemical nature[46], the experimental and calculated values of q_m were not coherent with each other in this case. Therefore, it can be expressed that D–R adsorption isotherm is not properly suited for these system. According to the comparative results obtained from the Langmuir, Freundlich, and D–R adsorption isotherm models, it is concluded that the adsorption of Pb(II) ions onto HDMS and ODMS from aqueous solution was determined to be suited well with the Langmuir isotherm which indicates the monolayer adsorption.

The results also showed that the polyphosphazene microspheres displayed considerable high adsorption capacity for Pb(II) ions by comparison with the other adsorbents reported in the literature (Table 3). Inorganic–organic hybrid polyphosphazenes possessing high cross-linked structure in the polymer matrices exhibit more active sites to the target metal ions comparing to traditional adsorbents. The stereochemical arrangement of N-donor atoms on polyphosphazene framework plays an important role in the adsorption of Pb(II) ions. The interactions between polymeric structure and metal ions are possible to be occurred via

Table 2. Adsorption isotherm parameters for the adsorption of Pb(II) ions onto HDMS and ODMS at 20 °C.

Adsorbent	Langmuir				Freundlich			Dubinin–Radushkevich (D–R)			
	q_{max} (mg g^{-1})	K_L (dm^3 mg^{-1})	r_L^2	R_L	K_F (dm^3 g^{-1})	n	r_F^2	q_m (mg g^{-1})	B (mol^2 kJ^{-2})	r_{D-R}^2	E (kJ mol^{-1})
HMDS	157.4	6.07×10^{-2}	0.991	0.105	25.7	2.565	0.950	545.6	3.70×10^{-3}	0.961	11.6
OMDS	308.0	0.169	0.998	2.15×10^{-2}	107.3	4.252	0.811	1031	2.26×10^{-3}	0.818	14.9

Table 3. Adsorption results of Pb(II) ions from the literature by various adsorbents.

Adsorbent	Adsorption capacity (mg g^{-1})	pH	T (°C)	Initial metal ion concentration (mg dm^{-3})	Adsorbent amount (g dm^{-3})	Reference
Sol–gel derived organic–inorganic hybrid sorbent	66.3	6.0	25	50–900	1.0	[4]
Pb(II)-imprinted silica sorbent	61.9	4.5	25	150–850	4.0	[48]
Poly(ethyleneimine)-functionalized hybrid silica by hydrothermal heating	68.1	5.0	25	50–600	4.0	[49]
Tetrasulfide-functionalized silica gel	62.2	6.0	25	50–1000	2.0	[50]
PEI-functionalized hybrid sorbent	91.5	5.0	25	100–800	4.0	[51]
Diffusive gradients in thin films (DGT)-Pb(II) imprinted	69.1	5.0	25	100–800	NA	[52]
Poly(HEMA-co-DMAa)	70.5	<8.0	20	10–200	5.0	[53]
HDMS	157.4	5.5	20	75–250	0.5	This study
ODMS	308.0	5.5	20	75–250	0.5	This study

NA, not available.

unattached –NH$_2$ groups, –NH groups at the framework and N atoms on the phosphazene rings. According to the theory of hard and soft acids and bases, polyphosphazenes comprising N-donor atoms which are defined as borderline bases and Pb(II) ion is defined as a borderline acid, and they bind each other easily.[48]

Regeneration

Regeneration and reuse of adsorbents are important properties of adsorption process from economy and environmental point of view. The regenerated adsorbents were reused for up to four adsorption–desorption cycles. After cycles, the adsorption capacities of Pb(II) ions were found to be around 65% for HDMS and 78% for ODMS. The results indicated that the good regeneration capacities were obtained by ODMS.

Conclusions

The highly cross-linked polyphosphazene inorganic–organic hybrid HDMS and ODMS were successfully synthesized by a one-step precipitation polymerization technique and characterized by SEM, FTIR spectroscopy and DLS measurements. The adsorption abilities of HDMS and ODMS for the removal of Pb(II) ions from aqueous solutions were investigated by using batch system studies. The adsorptions of Pb(II) ions onto HDMS and ODMS were verified by the FTIR spectra. The particle sizes of Pb(II) loaded HDMS and ODMS were measured as 3.82 and 1.04 μm, respectively. The pH effect on the adsorption of Pb(II) ions was investigated and the optimum value for both adsorbents was determined as pH 5.5. The adsorption of Pb(II) ions onto HDMS and ODMS was not influenced by changing the temperature. Adsorption equilibrium times for HDMS and ODMS were found to be 15 and 50 min and the adsorption of Pb(II) ions onto both adsorbent fitted the pseudo-second-order kinetic model. The calculated maximum adsorption capacities by Langmuir isotherm model was 157.4 mg g^{-1} for HDMS and 308.0 mg g^{-1} for ODMS. The results indicated that ODMS have a great number of nitrogen atoms having lone-pair electrons and exhibits base behavior to donate electrons and interact with metal ions which are defined as Lewis acids and can be selectively adsorbed on the microspheres. Therefore, ODMS adsorbs target metal ions with a higher adsorption capacity than HDMS because of the nitrogen-enriched structure.[10]

Experimental

Materials and methods

HCCP (hexachlorocyclotriphosphazene, 99%, Sigma-Aldrich) and OCCP (octachlorocyclotetraphosphazene, 98%, Otsuka Chemical Co. Ltd.) were recrystallized from dry N-heptane before use. 4,4′-diaminodiphenylmethane (DADPM, ≥97.0%), triethylamine (TEA, ≥99%), acetonitrile (anhydrous, 99.8%), tetrahydrofuran (THF, anhydrous, ≥99.9%) and Pb(NO$_3$)$_2$

(≥99.0%) were purchased from Sigma-Aldrich and Merck Companies and were used without further purification.

Characterization of HDMS and ODMS

SEM images of HDMS and ODMS were performed on a ZEISS Ultra Plus model Scanning Electron Microscope. FTIR (Perkin Elmer Spectrum 100 spectrometer) was used to explain the functional groups of the microspheres. The surface areas of HDMS and ODMS were determined by using Methylene Blue method.[54] DLS measurements were also performed using a Zeta Sizer (Malvern ZEN 3600) for the determination of particle size distributions of microspheres.

Preparation of HDMS and ODMS

HDMS (poly(cyclotriphosphazene-co-4,4′-diaminodiphenylmethane) and ODMS (poly(cyclotetraphosphazene-co-4,4′-diaminodiphenylmethane) were synthesized using a self-assembly and one pot precipitation polymerization technique.[23–26] HCCP or OCCP and DADPM were dissolved in acetonitrile and poured into flasks, separately. The molar ratios of the crosslinker (HCCP: N$_3$P$_3$Cl$_6$, 0.663 mmol; OCCP: N$_4$P$_4$Cl$_8$, 0.465 mmol) and monomer DADPM (4,4′-diaminodiphenylmethane 2.652 mmol for HDMS; 0.465 mmol for ODMS) were selected as 1:4 for HDMS and 1:1 for ODMS on the basis of experience to obtain best morphologies. The excess amounts of TEA (33.2 mmol for HDMS; 23.2 mmol for ODMS) were added into both reaction media and the reaction mixtures were kept under ultrasonic power (100 W; 53 kHz) at 40 °C, for 3 h. The precipitated polyphosphazene microspheres were isolated by centrifugation (4000 rpm), washed with THF, water and ethanol, respectively. Finally, the powder product was dried under vacuum at 50 °C. The synthesis route and structures of prepared HDMS and ODMS polyphosphazene compounds are depicted in Figure 9.

Adsorption experiments

Adsorption experiments were carried out in a batch technique. The optimum pH was determined where the maximum adsorption occurred. 100 mg dm^{-3} Pb(II) ions solutions were treated with 0.5 g dm^{-3} of each adsorbents (HDMS and ODMS) in the 100 mL Erlenmeyer flasks and then the pH of solutions was regulated between 1.0 and 6.0 by adding a small volume of HCl or acetate buffer solution using a pH meter (Radiometer Analytical MeterLab pHM 220). The mixtures were stirred at a constant temperature (20 °C) for 60 min until the equilibrium was established. The mixtures were then gently filtered and the concentrations of Pb(II) ions in solutions were analyzed by PerkinElmer Model AAnalyst 800 (Massachusetts, USA) flame atomic absorption spectrophotometer (AAS) with an air–acetylene flame. Deuterium background correction was done and the spectral slit width was 1.3 nm. The working wavelength was 283.3 nm. The instrument calibration was periodically tested for every 15 reading. The adsorbed amounts of Pb(II) ions for HDMS and ODMS were determined by the difference
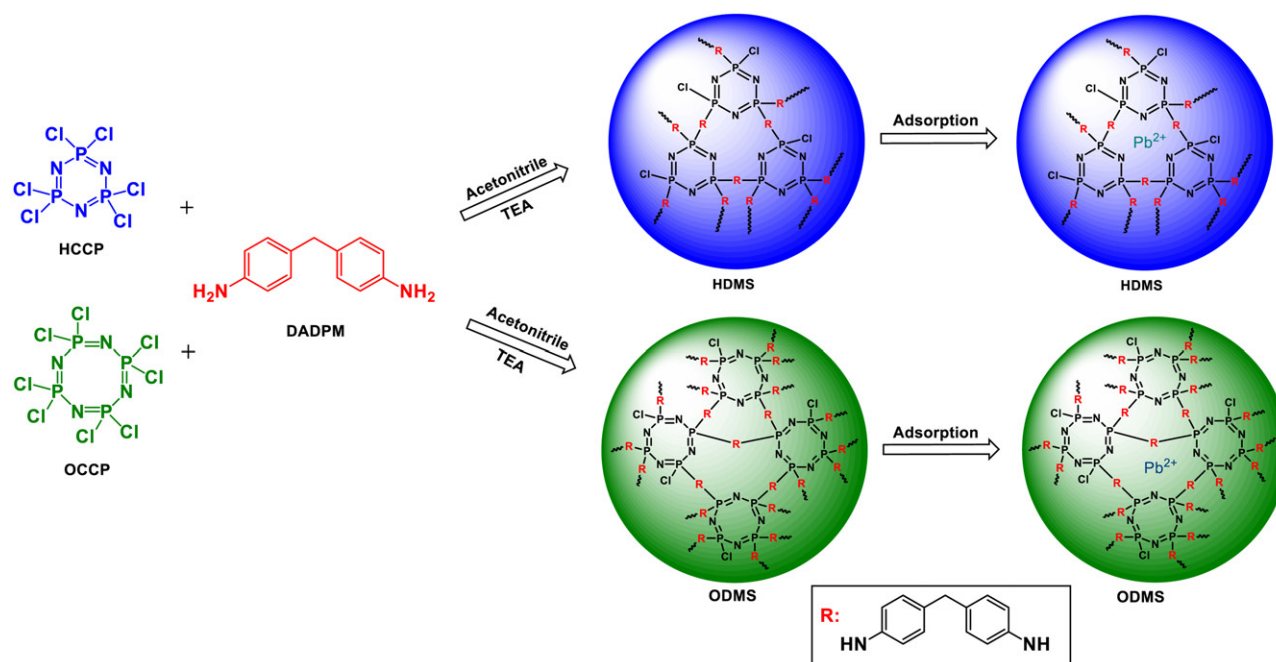
Figure 9. Suggested chemical structures and synthesis route of HDMS and ODMS.

between the initial and the remaining concentrations of Pb(II) ions in solution.

The adsorption experiments were also performed with time and concentration to assign the equilibrium time and the maximum removal. Kinetic studies were carried out by using $100\ mg\ dm^{-3}$ Pb(II) ions solution for both adsorbents. The concentration range for the isotherm studies was $75-250\ mg\ dm^{-3}$. The mixtures were magnetically stirred and kept in a water bath at $20\,°C$ and pH 5.5. After a definite time, the mixtures were filtered and the solutions were quantitatively analyzed by AAS to determine the adsorption of Pb(II) ions onto HDMS and ODMS.

Regeneration studies

The recovery and reusability of the adsorbent materials is an important issue related to the practical application of adsorption processes. In this study, HDMS and ODMS were subjected to 0.1 M HCl solution in order to determine desorption properties of adsorbents. The loaded Pb(II) ions were eluted in 50 mL (S/L = 0.5) of the eluent. Each adsorption and desorption cycle was enabled to interact for 60 min and consecutive adsorption–desorption cycles were repeated four times using the same adsorbent. The recovered adsorbent was washed repeatedly with deionized water to remove any desorbing solution and metal solution was poured into the adsorbent for the next adsorption cycle.

References

[1] Martinez, M.; Miralles, N.; Hidalgo, S.; Fiol, N.; Villaescusa, I.; Poch, J. Removal of Lead(II) and Cadmium(II) from Aqueous Solutions Using Grape Stalk Waste. *J. Hazard. Mater.* **2006**, *133*, 203–211. DOI: 10.1016/j.jhazmat.2005.10.030.

[2] Pagnanelli, F.; Esposito, A.; Toro, L.; Vegliò, F. Copper and Cadmium Biosorption onto *Sphaerotilus natans*: Application and Discrimination of Commonly Used Adsorption Models. *Sep. Sci. Technol.* **2002**, *37*, 677–699. DOI: 10.1081/SS-120001454.

[3] Ali, S.; Zuhra, Z.; Butler, I.-S.; Dar, S.-U.; Hameed, M.-U.; Wu, D.; Zhang, L.; Wu, Z. High-Throughput Synthesis of Cross-Linked Poly(Cyclotriphosphazene-Co-Bis(Aminomethyl)Ferrocene) Microspheres and Their Performance as a Superparamagnetic, Electrochemical, Fluorescent and Adsorbent Material. *Chem. Eng. J* **2017**, *315*, 448–458. DOI: 10.1016/j.cej.2017.01.049.

[4] Fan, H.-T.; Su, Z.-J.; Fan, X.-L.; Guo, M.-M.; Wang, J.; Gao, S.; Sun, T. Sol–Gel Derived Organic–Inorganic Hybrid Sorbent for Removal of Pb^{2+}, Cd^{2+} and Cu^{2+} from Aqueous Solution. *J. Sol-Gel Sci. Technol.* **2012**, *64*, 418–426. DOI: 10.1007/s10971-012-2872-x.

[5] Zhang, T.; Cai, Q.; Wu, D.-Z.; Jin, R.-G. Phosphazene Cyclomatrix Network Polymers: Some Aspects of the Synthesis, Characterization, and Flame-Retardant Mechanisms of Polymer. *J. Appl. Polym. Sci.* **2005**, *95*, 880–889. DOI: 10.1002/app.21295.

[6] Orme, C. J.; Stewart, F. F. Mixed Gas Hydrogen Sulfide Permeability and Separation Using Supported Polyphosphazene Membranes. *J. Membr. Sci.* **2005**, *253*, 243–249. DOI: 10.1016/j.memsci.2004.12.034.

[7] Kim, J. K.; Toti, U. S.; Song, R.; Sohn, Y. S. A Macromolecular Prodrug of Doxorubicin Conjugated to a Biodegradable Cyclotriphosphazene Bearing a Tetrapeptide. *Biorg. Med. Chem. Lett.* **2005**, *15*, 3576–3579. DOI: 10.1016/j.bmcl.2005.05.057.

[8] Chang, F.; Huang, X.; Wei, H.; Chen, K.; Shan, C.; Tang, X. Intrinsically Fluorescent Hollow Spheres Based on Organic–Inorganic Hybrid Polyphosphazene Material: Synthesis and Application in Drug Release. *Mater. Lett.* **2014**, *125*, 128–131. DOI: 10.1016/j.matlet.2014.03.137.

[9] Liu, W.; Huang, X.; Wei, H.; Chen, K.; Gao, J.; Tang, X. Facile Preparation of Hollow Crosslinked Polyphosphazene Submicrospheres with Mesoporous Shells. *J. Mater. Chem.* **2011**, *21*, 12964–12968. DOI: 10.1039/c1jm11802a.

[10] Wei, W.; Lu, R.; Xie, H.; Zhang, Y.; Bai, X.; Gu, L.; Da, R.; Liu, X. Selective Adsorption and Separation of Dyes from an Aqueous Solution on Organic–Inorganic Hybrid Cyclomatrix Polyphosphazene Submicro-Spheres. *J. Mater. Chem. A* **2015**, *3*, 4314–4322. DOI: 10.1039/c4ta06444e.

[11] Fu, J.; Chen, Z.; Wu, X.; Wang, M.; Wang, X.; Zhang, J.; Zhang, J.; Xu, Q. Hollow Poly(Cyclotriphosphazene-Co-

Phloroglucinol) Microspheres: An Effective and Selective Adsorbent for the Removal of Cationic Dyes from Aqueous Solution. *Chem. Eng. J* **2015**, *281*, 42–52. DOI: 10.1016/j.cej.2015.06.088.

[12] Allcock, H. R.; Welker, M. F.; Parvez, M. Synthesis and Structure of Borazinylsubstituted Small-Molecule and High Polymeric Phosphazenes: Ceramic Precursors. *Chem. Mater.* **1992**, *4*, 296–307. DOI: 10.1021/cm00020a015.

[13] Zhang, X.; Ren, S.; Han, T.; Hua, M.; He, S. New Organic–Inorganic Hybrid Polymers as Pickering Emulsion Stabilizers. *Colloids Surf. A: Physicochem. Eng. Aspects* **2018**, *542*, 42–51. DOI: 10.1016/j.colsurfa.2018.01.034.

[14] Chen, Z.; Fu, J.; Wang, M.; Wang, X.; Zhang, J.; Xu, Q. Adsorption of Cationic Dye (Methylene Blue) from Aqueous Solution Using Poly(Cyclotriphosphazene-Co-4,4′-Sulfonyldiphenol)Nanospheres. *Appl. Surf. Sci.* **2014**, *289*, 495–501. DOI: 10.1016/j.apsusc.2013.11.022.

[15] Chen, Z.; Zhang, J.; Fu, J.; Wang, M.; Wang, X.; Han, R.; Xu, Q. Adsorption of Methylene Blue onto Poly(Cyclotriphosphazene-Co-4,4-Sulfonyldiphenol) Nanotubes: Kinetics, Isotherm and Thermodynamics Analysis. *J. Hazard. Mater.* **2014**, *273*, 263–271. DOI: 10.1016/j.jhazmat.2014.03.053.

[16] Rekha, P.; Sharma, V.; Mohanty, P. Synthesis of Cyclophosphazene Bridged Mesoporous Organosilica for CO_2 Capture and Cr(VI) Removal. *Microporous Mesoporous Mater.* **2016**, *219*, 93–102. DOI: 10.1016/j.micromeso.2015.07.032.

[17] Huang, Z.; Chen, S.; Lu, X.; Lu, Q. Water-Triggered Self-Assembly Polycondensation for the One-Pot Synthesis of Cyclomatrix Polyphosphazene Nanoparticles from Amino Acid Ester. *Chem. Commun.* **2015**, *51*, 8373–8376. DOI: 10.1039/c5cc00735f.

[18] Chen, C.; Zhu, X.-Y.; Gao, Q.-L.; Fang, F.; Wang, L.-W.; Huang, X.-J. Immobilization of Lipase onto Functional Cyclomatrix Polyphosphazene Microspheres. *J. Mol. Catal. B: Enzym.* **2016**, *132*, 67–74. DOI: 10.1016/j.molcatb.2016.07.003.

[19] Ozay, H.; Ozay, O. Synthesis and Characterization of Drug Microspheres Containing Phosphazene for Biomedical Applications. *Colloids Surf. A: Physicochem. Eng. Aspects* **2014**, *450*, 99–105. DOI: 10.1016/j.colsurfa.2014.03.022.

[20] Ake, C. L.; Mayura, K.; Huebner, H.; Bratton, G. R.; Phillips, T. D. Development of Porous Clay-Based Composıtes for the Sorptıon of Lead from Water. *Toxicol. Environ. Health A* **2001**, *63*, 459–475. DOI: 10.1080/152873901300343489.

[21] Environmental Protection Agency, U. S. National Primary Drinking Water Regulations for Lead and Copper. *Federal Register* **1988**, *53*, 31515–31578.

[22] Singh, S.; Ma, L.; Hendry, M. Characterization of Aqueous Lead Removal by Phosphatic Clay: Equilibrium and Kinetic Studies. *J. Hazard. Mater.* **2006**, *136*, 654–662. DOI: 10.1016/j.jhazmat.2005.12.047.

[23] Zhang, P.; Huang, X.; Fu, J.; Huang, Y.; Zhu, Y.; Tang, X. A One-Pot Approach to Novel Cross-Linked Polyphosphazene Microspheres with Active Amino Groups. *Macromol. Chem. Phys.* **2009**, *210*, 792–798. DOI: 10.1002/macp.200800597.

[24] Wang, Y.; Mu, J.; Li, L.; Shi, L.; Zhang, W.; Jiang, Z. Preparation and Properties of Novel Fluorinated Crosslinked Polyphosphazene Micro-Nano Spheres. *High Perform Polym.* **2012**, *24*, 229–236. DOI: 10.1177/0954008311436221.

[25] Süzen, Y.; Metinoğlu, S. Synthesis and Characterization of Novel Inorganic and Organic Hybrid Poly[Cyclotriphosphazene-Co-(4,4′-Diaminophenylmethane)] Microspheres via One-Pot Self-Assembly Polycondensation Approach. *JOTCSA* **2016**, *3*, 167–182. DOI: 10.18596/jotcsa.36886.

[26] Süzen, Y.; Metinoğlu, S. Ö. Novel Cyclomatrix-Type Polyphosphazene Microspheres Crosslinked with Octachlorocyclo-tetraphosphazene: Preparation and Characterization. *Anadolu Univ. J. Sci. Technol. A: Appl. Sci. Eng.* **2017**, *18*, 973–987. DOI: 10.18038/aubtda.312012.

[27] Wang, M.; Fu, J.; Chen, Z.; Wang, X.; Xu, Q. In Situ Growth of Gold Nanoparticles onto Polyphosphazene Microspheres with Amino-Groups for Alcohol Oxidation in Aqueous Solutions. *Mater. Lett.* **2015**, *143*, 201–204. DOI: 10.1016/j.matlet.2014.12.114.

[28] Chen, K.; Huang, X.; Wan, C.; Liu, H. Heteroatom-Doped Mesoporous Carbon Nanofibers Based on Highly Cross-Linked Hybrid Polymeric Nanofibers: Facile Synthesis and Application in an Electrochemical Supercapacitor. *Mater. Chem. Phys.* **2015**, *164*, 85–90. DOI: 10.1016/j.matchemphys.2015.08.027.

[29] Beşli, S.; Mutlu, C.; İbişoğlu, H.; Yüksel, F.; Allen, C. W. Synthesis of a New Class of Fused Cyclotetraphosphazene Ring Systems. *Inorg. Chem.* **2015**, *54*, 334–341. DOI: 10.1021/ic5025235.

[30] Zhu, X.; Liang, Y.; Zhang, D.; Wang, L.; Ye, Y.; Zhao, Y. Synthesis and Characterization of Side Group–Modified Cyclotetra-phosphazene Derivatives. *Phosphorus Sulfur Silicon Relat. Elem.* **2011**, *186*, 281–286. DOI: 10.1080/10426507.2010.496120.

[31] Stuart, B. *Infrared Spectroscopy: Fundamentals and Applications*; John Wiley and Sons. Ltd: New York, **2004**, ISBNs: 0-470-85428-6 (PB).

[32] Özcan, A. S.; Gök, Ö.; Özcan, A. Adsorption of Lead(II) Ions onto 8-Hydroxy Quinoline-Immobilized Bentonite. *J. Hazard. Mater.* **2009**, *161*, 499–509. DOI: 10.1016/j.jhazmat.2008.04.002.

[33] Lagergren, S. K. About the Theory of so-Called Adsorption of Soluble Substance. *Sven. Vetenskapsakad. Handingar* **1898**, *24*, 1–39.

[34] Ho, Y. S.; McKay, G. Kinetic Models for the Sorption of Dye from Aqueous Solution by Wood. *Process Saf. Environ. Prot.* **1998**, *76*, 183–191. DOI: 10.1205/095758298529326.

[35] Azizian, S. Kinetic Models of Sorption: A Theoretical Analysis. *J. Colloid Interface Sci.* **2004**, *276*, 47–52. DOI: 10.1016/j.jcis.2004.03.048.

[36] Elovich, S. J. In Proceedings of the Second International Congress of Surface Activity, Butterworths Scientific Publications: London, **1957**.

[37] Weber, W. J.; Morris, J. C. Kinetics of Adsorption Carbon from Solutions. *J. Sanitary Eng. Div. Am. Soc. Civ. Eng.* **1963**, *89*, 31–60.

[38] Tanhaei, B.; Ayati, A.; Lahtinen, M.; Sillanpää, M. Preparation and Characterization of a Novel Chitosan/Al$_2$O$_3$/Magnetite Nanoparticles Composite Adsorbent for Kinetic, Thermodynamic and Isotherm Studies of Methyl Orange Adsorption. *Chem. Eng. J.* **2015**, *259*, 1–10. DOI: 10.1016/j.cej.2014.07.109.

[39] Langmuir, I. The Adsorption of Gases on Plane Surfaces of Glass, Mica and Platinum. *J. Am. Chem. Soc.* **1918**, *40*, 1361–1403. DOI: 10.1021/ja02242a004.

[40] Weber, T. W.; Chakravorti, R. K. Pore and Solid Diffusion Models for Fixed-Bed Adsorbers. *AIChE J.* **1974**, *20*, 228–238. DOI: 10.1002/aic.690200204.

[41] Hall, K. R.; Eagleton, L. C.; Acrivos, A.; Vermeulen, T. Pore- and Solid-Diffusion Kinetics in Fixed-Bed Adsorption under Constant-Pattern Conditions. *Ind. Eng. Chem. Fund.* **1966**, *5*, 212–223. DOI: 10.1021/i160018a011.

[42] Freundlich, H. Uber Die Adsorption in Losungen. *J. Phys. Chem.* **1906**, *57*, 385–470.

[43] Dubinin, M. M.; Radushkevich, L. V. Equation of the Characteristic Curve of Activated Charcoal. *Proc. Acad. Sci. USSR Phys. Chem. Sect.* **1947**, *55*, 331–333.

[44] Hobson, J. P. Physical Adsorption Isotherms Extending from Ultrahigh Vacuum to Vapor Pressure. *J. Phys. Chem.* **1969**, *73*, 2720–2727.

[45] Hasany, S. M.; Chaudhary, M. H. Sorption Potential of Haro River Sand for the Removal of Antimony from Acidic Aqueous Solution. *Appl. Radiat. Isot.* **1996**, *47*, 467–471.

[46] Helfferich, F. G. *Ion Exchange Chromatography*, McGraw-Hill: New York, **1962**. DOI: 10.1126/science.138.3537.133.

[47] Onyango, M. S.; Kojima, Y.; Aoyi, O.; Bernardo, E. C.; Matsuda, H. Adsorption Equilibrium Modeling and Solution

Chemistry Dependence of Fluoride Removal from Water by Trivalent-Cation-Exchanged Zeolite F-9. *J. Colloid Interface Sci.* **2004**, *279*, 341–350. DOI: 10.1016/j.jcis.2004.06.038.

[48] Fan, H. T.; Sun, X. T.; Zhang, Z. G.; Li, W. X. Selective Removal of Lead(II) from Aqueous Solution by an Ion-Imprinted Silica Sorbent Functionalized with Chelating N-Donor Atoms. *J. Chem. Eng. Data* **2014**, *59*, 2106–2114. DOI: 10.1021/je500328t.

[49] He, L.; Liu, D.-D.; Wang, B.-B.; Xu, H.-B. Adsorption of Lead(II) from Aqueous Solution Using a Poly(Ethyleneimine)-Functionalized Organic–Inorganic Hybrid Silica Prepared by Hydrothermal-Assisted Surface Grafting Method. *Asia-Pac. J. Chem. Eng.* **2014**, *9*, 800–809. DOI: 10.1002/apj.1823.

[50] Fan, H. T.; Wu, J. B.; Fan, X. L.; Zhang, D. S.; Su, Z. J.; Yan, F.; Sun, T. Removal of Cadmium(II) and Lead(II) from Aqueous Solution Using Sulfur-Functionalized Silica Prepared by Hydrothermal-Assisted Grafting Method. *Chem. Eng. J.* **2012**, *198–199*, 355–363. DOI: 10.1016/j.cej.2012.05.109.

[51] He, L.; Liu, D.-D.; Wang, B.-B.; Liu, N. Poly(Ethyleneimine)-Functionalized Silica-Supported Organic–Inorganic Hybrid Sorbent Prepared by Combining Sol–Gel Method and Hydrothermal-Assisted Process. *Chem. Lett.* **2014**, *43*, 579–581. DOI: 10.1246/cl.131067.

[52] Sui, D.-P.; Chen, H.-X.; Liu, L.; Liu, M.-X.; Huang, C.-C.; Fan, H.-T. Ion-Imprinted Silica Adsorbent Modified Diffusive Gradients in Thin Films Technique: Tool for Speciation Analysis of Free Lead Species. *Talanta* **2016**, *148*, 285–291. DOI: 10.1016/j.talanta.2015.11.003.

[53] Ramos-Jacques, A. L.; Lujan-Montelongo, J. A.; Silva-Cuevas, C.; Cortez-Valadez, M.; Estevez, M.; Hernandez-Martínez, A. R. Lead (II) Removal by Poly(*N*,*N*-Dimethylacrylamide-Co-2-Hydroxyethyl Methacrylate). *Eur. Polym. J.* **2018**, *101*, 262–272. DOI: 10.1016/j.eurpolymj.2018.02.032.

[54] Hang, P. T.; Brindley, G. Methylene Blue Absorption by Clay Minerals. Determination of Surface Areas and Cation Exchange Capacities (Clay-Organic Studies XVIII). *Clays Clay Mine* **1970**, *18*, 203–212.